

Synthesis, Structure, and Characterization of N-Ligated $W_6S_8L_6$ Cluster Complexes

Grant M. Ehrlich,[†] Christopher J. Warren,[†] Deborah A. Vennos,[†] Douglas M. Ho,[‡] Robert C. Haushalter,[§] and Francis J. DiSalvo^{*,†}

Department of Chemistry, Cornell University, Ithaca, New York 14853-1301, Department of Chemistry, Princeton University, Princeton, New Jersey 08544, and NEC Research Institute, 4 Independence Way, Princeton, New Jersey 08540

Received March 2, 1995[⊗]

The synthesis and structure determination of two N-ligated $W_6S_8L_6$ ($L = \text{pyridine}$ or $4\text{-tert-butylpyridine}$) complexes are presented. Described herein is the preparation of $W_6S_8(C_5H_5N)_6$ (**1**) from the reaction of W_6Cl_{12} , NaSH, and NaOBu in refluxing pyridine and the preparation of $W_6S_8(C_9H_{13}N)_6 \cdot 6C_6H_6$ (**2**) from the reaction of W_6Cl_{12} , KSH, KOBu, and $4\text{-tert-butylpyridine}$ in DMF (followed by recrystallization from benzene). Thin, orange plate-shaped crystals of $W_6S_8(C_5H_5N)_6$ (**1**) were isolated after working up the product from the above reaction in pyridine at 210 °C. They crystallize in the space group $P\bar{1}$ (No. 2) with lattice constants $a = 9.404(2)$ Å, $b = 10.725(5)$ Å, $c = 11.905(6)$ Å, $\alpha = 114.43(3)^\circ$, $\beta = 90.52(3)^\circ$, $\gamma = 109.07(3)^\circ$, $V = 1018.6(7)$ Å³, and $Z = 1$, with R (R_w) = 0.0525 (0.0686). Large, dark red-brown crystals of $W_6S_8(C_9H_{13}N)_6 \cdot 6C_6H_6$ (**2**) were prepared by a method similar to that for **1**, but under less rigorous conditions. This method leads to the isolation of $W_6S_8(C_9H_{13}N)_6 \cdot 6C_6H_6$ (**2**), which crystallizes in the space group $R\bar{3}$ (No. 148) with lattice constants $a = 20.208(3)$ Å, $c = 20.843(3)$ Å, $V = 7371(2)$ Å³, and $Z = 3$, with R (R_w) = 0.0413 (0.0482). Both **1** and **2** contain the neutral, substitution-resistant W_6S_8 cluster core consisting of an octahedral arrangement of tungsten atoms with face-capping sulfur atoms. The coordination environment of each tungsten atom is completed by a single pyridine (or $4\text{-tert-butylpyridine}$) ligand in the *exo* position. All of the W–W and W–S distances in these clusters fall within the ranges 2.652–2.667 Å (for W–W) and 2.430–2.478 Å (for W–S), which are comparable to those found in related tungsten sulfide cluster complexes.

Introduction

Some of the earliest group 6 M_6S_8 molecular clusters to be characterized were $Mo_6S_8(PEt_3)_6$ and $W_6S_8(PEt_3)_6$.^{1,2} Since their preparation, it has been recognized that molecular W_6S_8 clusters have the potential of being precursors to the elusive tungsten Chevrel phases.³ These phosphine-ligated clusters have been prepared by the reductive dimerization of the trinuclear cluster $Mo_3S_7Cl_4$ or $W_3S_7Cl_4$ with Mg in the presence of triethylphosphine. We have found that this method of preparing M_6S_8 cluster complexes is difficult because it requires multiple steps [including the presynthesis of $X_3S_7Cl_4$ ($X = Mo, W$)] and the magnesium metal must be particularly clean and finely divided or no reaction occurs. The yields in these syntheses are also relatively low. For example, Saito et al. report that $Mo_6S_8(PEt_3)_6$ may be prepared in 32% yield^{1b} and, similarly, the preparation of $W_6S_8(PEt_3)_6$ is reported in only 10% yield.² The phosphine ligands in these complexes are also strongly bound, making

possible substitutions with other, more desirable ligands unlikely. Since we are interested in producing a wide variety of ligated and linked metal clusters with potentially weak donors such as pyrazine, we have been investigating reactions in which donors weaker than triethylphosphine can be bound to the W_6S_8 cluster. Such a weakly bound ligand would be desirable if these complexes are to be used as intermediates to extended Chevrel-like W_6S_8 structures.

More recently, other M_6S_8 clusters have been prepared using NaSH and the metal dichloride.^{4–6} These efforts have shown that NaSH can be used for the stepwise displacement of chloride by sulfide in $M_6X_8^{4+}$ clusters ($M = Mo, W$; $X = Cl, Br$) by stirring in either refluxing pyridine, pyrrolidine, or piperidine, leading to completely sulfided products such as $Mo_6S_8(C_5H_5N)_6 \cdot 2C_5H_5N$, $Mo_6S_8(C_4H_9N)_6 \cdot C_4H_9N$, and $Mo_6S_8(C_5H_{11}N)_6 \cdot 7C_5H_{11}N$.⁴ Interestingly, intermediates such as $(C_5H_5NH)_3[(Mo_6Cl_7S)Cl_6]$ have also been characterized in these syntheses.⁷

Presented herein are the preparation and the structure determinations of two N-ligated W_6S_8 cluster complexes, $W_6S_8(C_5H_5N)_6$ (**1**) and $W_6S_8(C_9H_{13}N)_6 \cdot 6C_6H_6$ (**2**). By the methods described, bulk polycrystalline $W_6S_8(C_5H_5N)_6$ (**1**) may be obtained in greater than 43% yield, and a crystalline derivative of $W_6S_8(C_9H_{13}N)_6 \cdot 6C_6H_6$ (**2**) can be obtained in 35–40% yields.

Experimental Section

General Details. All manipulations were performed either under vacuum or in a purified Ar atmosphere, unless explicitly stated. Ether, THF, pentane, hexane, toluene, and benzene were stored over sodium/

* To whom correspondence should be addressed.

[†] Cornell University.

[‡] Princeton University.

[§] NEC Research Institute.

[⊗] Abstract published in *Advance ACS Abstracts*, July 15, 1995.

- (a) Saito, T.; Yamamoto, N.; Yamagata, T.; Imoto, H. *J. Am. Chem. Soc.* **1988**, *110*, 1646. (b) Saito, T.; Yamamoto, N.; Nagase, T.; Tsuboi, T.; Kobayashi, K.; Yamagata, T.; Imoto, H.; Unoura, K. *Inorg. Chem.* **1990**, *29*, 764.
- Saito, T.; Yoshikawa, A.; Yamagata, T.; Imoto, H.; Unoura, K. *Inorg. Chem.* **1989**, *28*, 3588.
- For a discussion of Chevrel phases and their properties see: (a) Chevrel, R.; Hirrien, M.; Sergent, M. *Polyhedron* **1986**, *5*, 87. (b) Chevrel, R.; Gougeon, P.; Potel, M.; Sergent, M. *J. Solid State Chem.* **1985**, *57*, 25. (c) Chevrel, R.; Sergent, M. In *Topics in Current Physics*; Maple, M. B.; Fischer, O., Eds.; Springer-Verlag: Berlin, 1982; Vol. 32, Chapter 2. (d) *Superconductivity in Ternary Compounds I*; Maple, M. B.; Fischer, O., Eds.; Springer-Verlag: Berlin, 1982. (f) Fischer, O. *Appl. Phys.* **1978**, *16*, 1. (e) Chevrel, R.; Sergent, M.; Prigent, J. *J. Solid State Chem.* **1971**, *3*, 515.

(4) Hilsenbeck, S. J.; Young, V. G., Jr.; McCarley, R. E. *Inorg. Chem.* **1994**, *33*, 1822.

(5) Spink, D. *Energy Res. Abstr.* **1990**, *15* (24), Abstr. No. 53377.

(6) (a) Zhang, X. Ph.D. Dissertation, Iowa State University, Ames, IA, 1991. (b) Hilsenbeck, S. Ph.D. Dissertation, Iowa State University, Ames, IA, 1990.

(7) Michel, J. B.; McCarley, R. E. *Inorg. Chem.* **1982**, *21*, 1864.

benzophenone and distilled prior to use. Pyridine (Fisher) was distilled from and stored over CaH_2 (Aldrich). DMF was stored over 4A molecular sieves and syringe-filtered through a 0.45 μm Teflon filter prior to use. Methanol (Fisher) was distilled from Mg/I_2 and stored over 3A molecular sieves. Ethanol was distilled from and stored over 3A molecular sieves. The molecular sieves were activated by heating to 400 °C in vacuo. Solution NMR spectra were obtained on a Varian VXR-400S NMR and solids NMR spectra were obtained on an IBM/Bruker AF-300 NMR spectrometer. Chemical shifts are reported downfield from $Si(Me)_4$. IR spectra were obtained on a Mattson FTIR (model IR-10410) spectrophotometer. All samples were prepared for IR analysis as KBr pellets. SEM/microprobe analysis was performed on a JEOL 733 Superprobe using the vendor supplied SSQ or SQ package for standardless semiquantitative elemental analysis. Unless explicitly stated, the contributions from light elements ($Z < 11$) were ignored. X-ray powder diffraction patterns were collected on a Scintag XDS-2000 diffractometer using $Cu K\alpha$ radiation. Simulated powder patterns were calculated using the McLazy program.⁸ Single-crystal X-ray diffraction data were collected on either a Syntex P2₁, a Siemens P4, or a Rigaku AFC7R diffractometer (see text for details), and the structures were solved and refined with either the SHELXTL or TEXSAN software package.⁹

Starting Materials. Anhydrous sodium hydrogen sulfide was prepared according to the method of Eibeck¹⁰ by the reaction of sodium ethoxide [prepared from sodium (10.0 g, 0.435 mol) and ethanol (200 mL)] and H_2S (Matheson, CP grade) which was dried over P_2O_5 (Aquasorb). Potassium hydrogen sulfide was prepared in a manner similar to the preparation of NaSH in which potassium (20.3 g, 0.519 mol) was dissolved in EtOH (200 mL, 3.4 mol) and the solution was bubbled with H_2S for 2 h. After the mixture was cooled to 0 °C, ether (300 mL) was added and the product collected by filtration. Anhydrous sodium butoxide was prepared from the reaction of sodium and butanol. Anhydrous potassium butoxide and 4-*tert*-butylpyridine were purchased from Aldrich. The 4-*tert*-butylpyridine was dried over CaH_2 at 110 °C for 6 h and distilled under reduced pressure prior to use, while the KOBu was used as obtained. W_6Cl_{12} was prepared from the reaction of W and WCl_6 .¹¹ Due to the violent nature of this reaction, it is described below in detail.

Preparation of W_6Cl_{12} . Impure 12 μm tungsten metal powder (Cerac) was purified at 800 °C under a stream of H_2/N_2 to remove trace amounts of the oxide. Tungsten(VI) chloride (Strem) was purified by sublimation, the more volatile impurities subliming below 190 °C, leaving cleaner W_6Cl_{12} , which was sublimed from the less volatile impurities at 240 °C. Purple tungsten(VI) chloride [24 g (0.06 mol)] and an excess of tungsten metal powder [25 g (0.14 mol)] were loaded into a 33 cm long, 26 mm i.d. quartz tube which had a 30° bend. The tube was sealed under vacuum and three-fourths of it was inserted into a tube furnace. The furnace was ramped from 25 to 270 °C over 3 h to distill the WCl_6 into the bent end of the tube, which hung outside the furnace. The furnace was then heated to 750 °C, and the tube was inserted into the furnace 1 cm every 15 min until the tungsten(VI) chloride melted and began to reflux. After 6 h, the reaction slowed and further insertion of the reaction tube was necessary to drive the reaction to completion. When the reaction was complete, impurities such as WCl_4 or $WOCl_4$ were sublimed from the product by heating the end of the tube containing the product at 450 °C for 2 h. The product was worked up in air by dissolving the impure W_6Cl_{12} in 100 mL of hot 6 M HCl and filtering through a coarse frit using the filter aid Celite (diatomaceous earth). The frit was washed three times with boiling 6 M HCl. The volume of the filtrate was reduced until the product began to crystallize. The volume was then tripled with 12 M HCl and the mixture was cooled to -10 °C. The yellow green needles of $(H_3O)_2[W_6Cl_{14}] \cdot 6 H_2O$ which grew from the solution were recovered and washed with cold 6 M HCl. The hydrate was dried in vacuo by

ramping to 300 °C at no more than 100 °C/h and holding at 300 °C for 1 h to yield a brown amorphous product. The yield was 16.5 g (35.7%). The powder pattern of the hydrate, $(H_3O)_2[W_6Cl_{14}] \cdot 6 H_2O$, has peaks at d (Å) = 7.11, 6.36, 2.78, 2.54, 2.35, 2.01, and 1.89. The dried product obtained at 300 °C is amorphous and does not exhibit Bragg scattering. However, broad peaks attributable to crystalline W_6Cl_{12} are observed at d (Å) = 6.94, 5.63, 2.88, 2.61, 2.19, and 2.07 upon further heating and sintering of the product at 450 °C.

Synthesis of $W_6S_8(C_5H_5N)_6$. Using a modification of a procedure first discussed by McCarley at a meeting of the American Chemical Society¹² and recently available in a Ph.D. dissertation,^{6a} crude $W_6S_8(C_5H_5N)_6$ (**1**) was prepared as follows: W_6Cl_{12} was dried to 425 °C. Both the sodium hydrogen sulfide and sodium butoxide appeared white, dry, and polycrystalline. In pyridine, tungsten dichloride (2.29 g, 8.98 mmol), sodium hydrogen sulfide (1.26 g, 22.5 mmol), and sodium butoxide (0.865 g, 9.0 mmol) were refluxed at 115 °C in an excess of pyridine for 4 days under dry nitrogen. The red-brown mixture was filtered, and the solid was washed twice with pyridine, seven times with 25 mL of dry MeOH, and dried in vacuo to yield a brown powder. The yield was 1.19 g (0.648 mmol, 43.3%). Using potassium butoxide instead of sodium butoxide in this preparation gave the desired product in similar yields. At 25 °C, $W_6S_8(C_5H_5N)_6$ (**1**) was found to be insoluble not only in pyridine but also in CH_3CN , MeOH, benzene, toluene, and hexane.

Although insoluble in pyridine at room temperature, $W_6S_8(C_5H_5N)_6$ (**1**) is slightly soluble in pyridine at elevated temperatures. X-ray-quality single crystals were grown by cooling the crude product (60 mg) slowly in pyridine (5 mL) in a sealed Pyrex tube from 210 °C at no greater than 1 °C/h. The orange plate-like crystals that formed were stable in air. $W_6S_8(C_5H_5N)_6$ (**1**) was characterized by ¹³C CPMAS solids NMR, elemental analysis via EDAX (energy dispersive analysis by X-rays), X-ray powder diffraction, and a single-crystal X-ray structure analysis. Three unique carbon resonances were observed in the ¹³C CPMAS NMR spectrum of the solid spinning at 3800 Hz at δ 123, 135, and 156, and spinning sidebands were observed at intervals of about 50 ppm from these resonances. For reference, ¹³C solution NMR of pyridine ($CDCl_3$) shows δ 123.7 (meta), 135.7 (para), and 149.9 (ortho).¹³ Microprobe analysis gave the expected ratio of W to S using the program SQ and the ZAF method with C fixed at 20 wt % and N fixed at 5 wt %. The accelerating voltage was 10 kV, and the tungsten M and sulfur K lines were used. Anal. Found (calcd) for $W_6S_8(C_5H_5N)_6$: W, 61.20 (60.14); S, 13.80 (13.98). No sodium or chlorine was observed in the EDAX spectrum.

Synthesis of $W_6S_8(C_9H_{13}N)_6 \cdot 6C_6H_6$. A 250 mL one-neck flask fitted with a connecting adapter was loaded with tungsten dichloride (0.600 g, 2.35 mmol), potassium hydrogen sulfide (0.558 g, 7.73 mmol), and potassium butoxide (0.529 g, 4.71 mmol). DMF (10 mL) was added through a syringe filter, and an excess of 4-*tert*-butylpyridine (0.50 mL, 3.38 mmol) was added by syringe.¹⁴ After stirring at 25 °C for 6 days, 100 mL of a 1:2 mixture of THF and hexanes was added to the dark brown product mixture and the contents of the flask were strained through a fine-porosity fritted funnel to yield a dark red liquid. Upon removal of less than one-third of the solvent under vacuum, orange needle-shaped crystals (unsuitable for single-crystal X-ray analysis due to their size and morphology) precipitated from the solution (yield = 36.9%). These orange crystals were analyzed via IR, ¹H NMR, and EDAX. The EDAX analysis of the crystals showed the presence of W and S (in an approximate 3:4 ratio). No potassium or chlorine was observed in the product by microprobe analysis. The ¹H NMR (C_6D_6) gave δ 1.35 (s, methyls), 6.64 (d, meta), and 9.87 (d, ortho). For comparison, ¹H NMR of 4-*tert*-butylpyridine (C_6D_6) shows peaks at δ 0.90 (s, methyls), 6.84 (d, meta), and 8.54 (d, ortho).¹⁵ The IR spectrum, taken as a KBr pellet, was similar to that of 4-*tert*-butylpyridine, with

(8) McLazy was obtained from Professor M. O'Keeffe, Department of Chemistry, Arizona State University, Tempe, AZ 85287.
 (9) (a) *TEXSAN Single Crystal Structure Analysis Software Package*, Version 1.6; Molecular Structure Corp.: The Woodlands, TX, 1993.
 (b) *SHELXTL PLUS 4.21 for Siemens Crystallographic Research Systems*; Siemens Analytical X-ray Instruments, Inc.: Madison, WI, 1990.
 (10) Eibeck, R. E. *Inorg. Synth.* **1963**, 7, 128 ff.
 (11) Ehrlich, G. M.; Rauch, P. E.; DiSalvo, F. J. *Inorg. Synth.*, in press.

(12) McCarley, R. E.; Zhang, X.; Spink, D. A.; Hur, N. Paper presented at the 199th National Meeting of the American Chemical Society, 1990.
 (13) Pouchert, C. J. *Aldrich Libr. NMR Spectra* **1983**, 2 (2), 611A.
 (14) It is interesting to note that, in the case of the pyridine-ligated cluster, the reaction is best when run in neat ligand in contrast to the case of the 4-*tert*-butylpyridine cluster, where better results were observed when a slight stoichiometric excess of the ligand was used in a DMF solution.
 (15) Pouchert, C. J.; Behnke, J. *Aldrich Libr. ¹³C ¹H FT-NMR Spectra* **1993**, 1 (3), 246B.

peaks at 2960, 1612, 1495, 1417, 1272, 828, 726, and 568 cm^{-1} . For comparison, 4-*tert*-butylpyridine exhibits IR bands at 2965, 1597, 1494, 1409, 1274, 821, 715, and 569 cm^{-1} .¹⁶ Both the IR and ¹H NMR spectra also exhibited peaks consistent with the presence of DMF molecules.

Large, dark red-brown prism-shaped crystals (0.5 mm on their longest edge) suitable for X-ray diffraction were grown by dissolving the crude orange crystals in either benzene at room temperature or neat 4-*tert*-butylpyridine sealed in a quartz tube and heated to 250 °C followed by slow cooling to room temperature.¹⁷ Crystals grown from a benzene solution contain six benzene molecules per $\text{W}_6\text{S}_8(\text{C}_9\text{H}_{13}\text{N})_6$ cluster and are present as solvates of crystallization. These crystals were found to be unstable, losing benzene on standing in the argon atmosphere of the glovebox, resulting in a discoloration of the crystal faces and complete decomposition of the crystals in a matter of minutes. The crystals obtained from the 4-*tert*-butylpyridine contained no solvent molecules and were stable in air. The product in each case was observed to be insoluble in pentane and hexane, sparingly soluble in acetonitrile, moderately soluble in toluene, and very soluble in benzene, DMF, THF, and DMSO.

X-ray Structure Determinations. $\text{W}_6\text{S}_8(\text{C}_5\text{H}_5\text{N})_6$. A dark orange platelike crystal of approximate dimensions $0.10 \times 0.05 \times 0.05$ mm was mounted on a glass fiber with epoxy cement and then transferred to a Syntex P2₁ diffractometer equipped with graphite-monochromated Mo K α radiation ($\lambda = 0.71073$ Å). Lattice parameters at 25 °C were determined from the setting angles of 25 carefully centered reflections having $15^\circ \leq 2\theta \leq 25^\circ$ and corresponded to a triclinic cell with the unit cell dimensions given in Table 1. Axial photographs and the lack of systematic absences in preliminary scans through reciprocal space were consistent with the triclinic space group $P\bar{1}$ (No. 2).

A full sphere of data ($\pm h, \pm k, \pm l$) within the 2θ range $3-45^\circ$ was collected with variable-speed $1.40^\circ 2\theta-\theta$ scans. A total of 3 check reflections were monitored after every 50 reflections during the data collection and showed no significant deviations from their mean intensity values. The 5360 measured reflections were corrected for Lorentz and polarization effects but not for extinction. An empirical absorption correction using the ψ -scan method was applied. An analytical absorption correction was also attempted, but found to be inferior to the ψ -scan method, most likely due to the difficulty of identifying and measuring the dominant faces in the oddly shaped crystal. Merging equivalents gave 2680 unique reflections ($R_{\text{int}} = 0.0305$) of which 2324 having $F > 4.0\sigma(F)$ were considered observed.

The structure was solved by direct methods and refined on F by full-matrix least-squares procedures using the Siemens SHELXTL PLUS program package. All of the non-hydrogen atoms were refined with anisotropic displacement coefficients. Hydrogen atoms were

Table 1. Crystallographic Data for $\text{W}_6\text{S}_8(\text{C}_5\text{H}_5\text{N})_6$ (**1**) and $\text{W}_6\text{S}_8(\text{C}_9\text{H}_{13}\text{N})_6 \cdot 6\text{C}_6\text{H}_6$ (**2**)

	1	2
chemical formula	$\text{W}_6\text{S}_8\text{C}_{30}\text{H}_{30}\text{N}_6$	$\text{W}_6\text{S}_8\text{C}_{90}\text{H}_{114}\text{N}_6$
fw	1834.19	2639.5
<i>a</i> , Å	9.404(2)	20.208(3)
<i>b</i> , Å	10.725(5)	20.208(3)
<i>c</i> , Å	11.905(6)	20.843(3)
α , deg	114.43(3)	90.0
β , deg	90.52(3)	90.0
γ , deg	109.07(3)	120.0
<i>V</i> , Å ³	1018.6(7)	7371(2)
<i>Z</i>	1	3
space group	$P\bar{1}$ (No. 2)	$R\bar{3}$ (No. 148)
ρ_{calcd} , g cm^{-3}	2.990	1.784
λ , Å	0.71073	0.71073
μ , cm^{-1}	176.70	72.07
<i>T</i> , °C	25	23
<i>R</i> ^a	0.0525	0.0413
<i>R</i> _w ^b	0.0686	0.0482

$$^a R = \sum(|F_o| - |F_c|) / \sum|F_o|. \quad ^b R_w = [(\sum w(|F_o| - |F_c|)^2) / \sum w|F_o|^2]^{1/2}.$$

Table 2. Atomic Coordinates ($\times 10^4$) and Equivalent Isotropic Displacement Coefficients ($\text{Å}^2 \times 10^3$) for $\text{W}_6\text{S}_8(\text{C}_5\text{H}_5\text{N})_6$ (**1**)

atom	<i>x</i>	<i>y</i>	<i>z</i>	<i>U</i> (eq) ^a
W(1)	1894(1)	1556(1)	5458(1)	22(1)
W(2)	9163(1)	1272(1)	6150(1)	21(1)
W(3)	9422(1)	472(1)	3750(1)	22(1)
S(1)	1984(5)	686(5)	3212(4)	31(2)
S(2)	454(5)	3060(4)	5354(4)	30(2)
S(3)	1515(5)	2204(5)	7636(4)	31(2)
S(4)	6982(5)	181(5)	4477(4)	30(2)
N(1)	4165(15)	3411(13)	5960(12)	30(6)
N(2)	8083(14)	2730(14)	7520(11)	30(6)
N(3)	8668(18)	1019(16)	2245(12)	40(8)
C(1)	5395(19)	3167(19)	5519(17)	41(8)
C(2)	6786(20)	4249(22)	5810(17)	46(10)
C(3)	6947(22)	5656(22)	6538(20)	56(11)
C(4)	5694(23)	5957(21)	7016(21)	57(10)
C(5)	4342(20)	4770(20)	6675(18)	48(9)
C(6)	8889(24)	4124(22)	8314(15)	51(10)
C(7)	8317(28)	5047(24)	9202(20)	68(12)
C(8)	6774(28)	4491(27)	9239(18)	67(13)
C(9)	5951(24)	3104(25)	8426(18)	55(12)
C(10)	6611(17)	2203(18)	7586(14)	36(8)
C(11)	8309(33)	2188(30)	2497(22)	93(18)
C(12)	7827(34)	2521(33)	1606(25)	89(19)
C(13)	7709(42)	1650(40)	401(30)	119(25)
C(14)	8035(42)	435(40)	91(25)	118(22)
C(15)	8463(39)	113(31)	1054(22)	104(20)

^a *U*(eq) is defined as one-third of the trace of the orthogonalized U_{ij} tensor.

included but not refined. The final least-squares refinement converged to R (R_w) = 0.0525 (0.0686) and $S = 1.09$ with 226 variables and 10.3 reflections per refined parameter. Further details of the X-ray structural analyses are given in Table 1. Atomic coordinates and equivalent isotropic displacement coefficients are given in Table 2, and selected interatomic distances and angles are given in Table 4.

$\text{W}_6\text{S}_8(\text{C}_9\text{H}_{13}\text{N})_6 \cdot 6\text{C}_6\text{H}_6$. A dark red-brown prism-shaped crystal of approximate dimensions $0.38 \times 0.50 \times 0.50$ mm was mounted in an inert argon atmosphere on a glass fiber with epoxy cement and then transferred to a Siemens P4 diffractometer equipped with graphite-monochromated Mo K α radiation ($\lambda = 0.71073$ Å). Lattice parameters at 23 °C were determined from the setting angles of 25 carefully centered reflections having $30^\circ \leq 2\theta \leq 38^\circ$ and corresponded to a trigonal cell with the unit cell dimensions given in Table 1. Systematic absences and intensity statistics obtained from preliminary scans through reciprocal space were consistent with the rhombohedral space group $R\bar{3}$ (No. 148).

Reflections in the $+h, +k, \pm l$ quadrant and within the 2θ range $4-50^\circ$ were collected with variable-speed $1.20^\circ \omega$ scans. A total of 3 check reflections were monitored after every 97 reflections during the data collection and showed no significant deviations from their mean

(16) Pouchert, C. J. *Aldrich Libr. FT-IR Spectra* **1985**, 1 (2), 736C.

(17) A red-brown needle-shaped crystal of approximate dimensions $0.25 \times 0.14 \times 0.14$ mm grown from neat 4-*tert*-butylpyridine (under the conditions described in the text) was analyzed via single-crystal X-ray diffraction on a Rigaku AFC7R four-circle diffractometer using graphite-monochromated Mo K α radiation and an 18 kW rotating anode generator. Crystal data for **3**: $\text{W}_6\text{S}_8\text{C}_{54}\text{H}_{78}\text{N}_6$, fw = 2170.83, tetragonal, space group $P4_2/n$ (No. 86), $a = 26.752(6)$ Å, $c = 9.436(3)$ Å, $V = 6752(1)$ Å³, $Z = 4$, and $\rho_{\text{calcd}} = 2.135$ g cm^{-3} . Cell constants were obtained at 25 °C using the setting angles of 25 carefully centered reflections in the range $20.32^\circ \leq 2\theta \leq 26.10^\circ$. Data collection consisted of scans of width $(0.84 + 0.35 \tan \theta)^\circ$ and were made at a speed of $16^\circ/\text{min}$ in the range $5^\circ \leq 2\theta \leq 60^\circ$. The 8051 measured reflections were corrected for Lorentz-polarization and absorption effects. Merging equivalents gave 7740 unique reflections ($R_{\text{int}} = 0.033$) of which 4407 having $I > 3.0\sigma(I)$ were considered observed. The structure was solved by direct methods and refined using the TEXSAN Crystal Structure Analysis Package of the Molecular Structure Corp. The refinements converged to R (R_w) = 0.028 (0.028) and $S = 1.36$ with 334 variables and 13.19 reflections per refined parameter. The structure is identical to that of $\text{W}_6\text{S}_8(\text{C}_9\text{H}_{13}\text{N})_6 \cdot 6\text{C}_6\text{H}_6$ (**2**) with the exception of the benzene solvate molecules (**3** contains no solvates of crystallization) and a slightly more pronounced canting of the 4-*tert*-butylpyridine ligands with respect to the W_6S_8 central cluster (e.g., rotated 8.1, 23.9, and 15.6° out of the W_4 planes [see Figure 3, bottom]). Like **2**, the solvent-free cluster exhibits a slight trigonal distortion, resulting this time in an *elongation* of the cluster in the direction normal to one of the W_3 faces. The W-W, W-S, and W-N bond distances in this cluster are consistent with those observed in **1** and **2**.

Table 3. Atomic Coordinates ($\times 10^4$) and Equivalent Isotropic Displacement Coefficients ($\text{\AA}^2 \times 10^3$) for $W_6S_8(C_9H_{13}N)_6 \cdot 6C_6H_6$ (**2**)

atom	x	y	z	$U(eq)^a$
W	182(1)	836(1)	519(1)	34(1)
S(1)	0	0	1439(2)	41(1)
S(2)	1539(1)	1205(1)	490(1)	42(1)
N(1)	395(4)	1853(4)	1121(3)	44(3)
C(2)	826(6)	2057(6)	1666(5)	61(5)
C(3)	944(6)	2655(6)	2040(5)	65(6)
C(4)	616(6)	3097(5)	1899(5)	54(5)
C(5)	182(6)	2889(5)	1349(5)	56(5)
C(6)	84(6)	2279(5)	985(5)	56(5)
C(7)	722(6)	3769(6)	2309(5)	68(6)
C(8a)	1238(13)	4503(10)	1947(11)	95(4)
C(9a)	1088(14)	3803(13)	2941(9)	95(4)
C(10a)	-48(10)	3692(14)	2459(12)	95(4)
C(8b)	1571(11)	4338(17)	2283(17)	95(4)
C(9b)	526(21)	3542(20)	3005(10)	95(4)
C(10b)	256(18)	4119(19)	2072(16)	95(4)
C(1sa)	1716(18)	480(11)	3437(12)	82(2)
C(2sa)	1383	528	2866	82(2)
C(3sa)	1842	980	2364	82(2)
C(4sa)	2635	1384	2432	82(2)
C(5sa)	2968	1335	3003	82(2)
C(6sa)	2509	884	3506	82(2)
C(1sb)	1528(14)	454(13)	3223(21)	82(2)
C(2sb)	1514	714	2606	82(2)
C(3sb)	2198	1201	2292	82(2)
C(4sb)	2895	1428	2595	82(2)
C(5sb)	2908	1168	3212	82(2)
C(6sb)	2224	681	3526	82(2)

^a $U(eq)$ is defined as one-third of the trace of the orthogonalized U_{ij} tensor.

intensity values. The 3177 measured reflections were corrected for Lorentz and polarization effects but not for absorption or extinction. Merging equivalents gave 2910 unique reflections ($R_{int} = 0.0425$) of which 2287 having $F > 3.0\sigma(F)$ were considered observed.

The structure was solved by heavy-atom methods and refined on F by full-matrix least-squares procedures using the Siemens SHELXTL PLUS program package. All of the non-hydrogen atoms were refined with anisotropic displacement coefficients (except where noted below). Hydrogen atoms were included but not refined. Both the *tert*-butyl group on the pyridine and the benzene molecule in the lattice were disordered and were treated with two-site disorder models. For the *tert*-butyl group, the two orientations of the methyls were specified by [C(8a), C(9a), C(10a)] and [C(8b), C(9b), C(10b)], mild distance restraints were applied, and one common isotropic displacement coefficient and one site occupancy parameter were refined. The latter yielded 59(1)% [C(8a), C(9a), C(10a)] and 41(1)% [C(8b), C(9b), C(10b)]. The benzene molecule was modeled with two overlapping regular hexagons refined as rigid groups with one common isotropic displacement coefficient and one site occupancy parameter [a, b = 55-(3)%, 45(3)%]. The final least-squares refinement converged to $R(R_w) = 0.0413$ (0.0482) and $S = 1.11$ with 119 variables and 19.2 reflections per refined parameter. Further details of the X-ray structural analysis are given in Table 1, final positional and equivalent isotropic displacement parameters are given in Table 3, and selected interatomic bond distances and angles are given in Table 5.

Large dark red-brown prismatic crystals obtained by recrystallization of the crude orange needles from 4-*tert*-butylpyridine in a sealed quartz tube at 250 °C were also analyzed by X-ray diffraction and found to contain the solvent-free cluster $W_6S_8(C_9H_{13}N)_6$ (**3**).¹⁷ The molecular structure of **3** is nearly identical to that of **2**, but with a slightly more pronounced canting of the pyridyl groups relative to the W_6S_8 core. Further details of the structure analysis of **3** are given in footnote 17.

Results and Discussion

In the course of our studies on M_6S_8 clusters and their potential use as precursors to new Chevrel phase materials,¹⁸ we noticed the development of a novel method for preparing

Table 4. Selected Bond Distances (\AA) and Angles (deg) in $W_6S_8(C_5H_5N)_6$ (**1**)^a

Bond Distances			
W(1)-W(2A)	2.665(2)	W(1)-W(3B)	2.667(2)
W(1)-W(2B)	2.654(2)	W(2A)-W(3A)	2.661(2)
W(1)-W(3A)	2.661(2)	W(2A)-W(3B)	2.662(2)
W(1)-S(1)	2.453(5)	W(2A)-S(3)	2.458(4)
W(1)-S(2)	2.458(6)	W(2A)-S(4A)	2.444(4)
W(1)-S(3)	2.454(4)	W(3A)-S(1)	2.460(5)
W(1)-S(4B)	2.449(6)	W(3A)-S(2)	2.473(4)
W(2A)-S(1A)	2.450(5)	W(3A)-S(3A)	2.478(4)
W(2A)-S(2)	2.460(5)	W(3A)-S(4A)	2.430(5)
W(1)-N(1)	2.257(11)	W(3A)-N(3A)	2.275(18)
W(2A)-N(2A)	2.258(14)		
Bond Angles			
W(2A)-W(1)-W(3A)	59.9(1)	W(1A)-W(2A)-W(3A)	60.2(1)
W(2A)-W(1)-W(3B)	59.9(1)	W(1B)-W(2A)-W(3B)	60.1(1)
W(2B)-W(1)-W(3A)	60.1(1)	W(1)-W(3A)-W(2A)	60.1(1)
W(2B)-W(1)-W(3B)	60.0(1)	W(1)-W(3A)-W(2B)	59.8(1)
W(1)-W(2A)-W(3A)	60.0(1)	W(1A)-W(3A)-W(2A)	59.7(1)
W(1)-W(2A)-W(3B)	60.1(1)	W(1A)-W(3A)-W(2B)	60.0(1)
W(2A)-W(1)-W(2B)	89.9(1)	W(3A)-W(2A)-W(3B)	90.2(1)
W(3A)-W(1)-W(3B)	90.1(1)	W(1)-W(3A)-W(1A)	89.9(1)
W(1)-W(2A)-W(1A)	90.1(1)	W(2A)-W(3A)-W(2B)	89.8(1)
S(1)-W(1)-S(2)	90.4(2)	S(2)-W(2A)-S(3)	88.8(2)
S(1)-W(1)-S(4B)	90.1(2)	S(2)-W(2A)-S(4A)	89.7(2)
S(2)-W(1)-S(3)	88.9(2)	S(1)-W(3A)-S(2)	89.9(1)
S(3)-W(1)-S(4B)	89.8(2)	S(1)-W(3A)-S(3A)	89.7(1)
S(1A)-W(2A)-S(3)	90.4(2)	S(2)-W(3A)-S(4A)	89.8(1)
S(1A)-W(2A)-S(4A)	90.3(2)	S(3A)-W(3A)-S(4A)	89.7(1)
S(1)-W(1)-S(3)	173.5(1)	S(3)-W(2A)-S(4A)	172.9(2)
S(2)-W(1)-S(4B)	172.8(1)	S(1)-W(3A)-S(4A)	172.9(2)
S(1A)-W(2A)-S(2)	173.6(2)	S(2)-W(3A)-S(3A)	172.3(2)
N(1)-W(1)-W(2A)	135.9(4)	N(2A)-W(2A)-W(3A)	135.2(4)
N(1)-W(1)-W(2B)	134.2(3)	N(2A)-W(2A)-W(3B)	134.6(4)
N(1)-W(1)-W(3A)	133.8(4)	N(3A)-W(3A)-W(1)	136.1(3)
N(1)-W(1)-W(3B)	136.1(4)	N(3A)-W(3A)-W(1A)	134.0(3)
N(2A)-W(2A)-W(1)	137.1(3)	N(3A)-W(3A)-W(2A)	134.5(4)
N(2A)-W(2A)-W(1A)	132.8(3)	N(3A)-W(3A)-W(2B)	135.7(4)
N(1)-W(1)-S(1)	92.0(4)	N(2A)-W(2A)-S(3)	94.5(3)
N(1)-W(1)-S(2)	93.0(4)	N(2A)-W(2A)-S(4A)	92.5(3)
N(1)-W(1)-S(3)	94.5(4)	N(3A)-W(3A)-S(1)	94.8(4)
N(1)-W(1)-S(4B)	94.2(4)	N(3A)-W(3A)-S(2)	94.1(4)
N(2A)-W(2A)-S(1A)	91.5(4)	N(3A)-W(3A)-S(3A)	93.6(4)
N(2A)-W(2A)-S(2)	94.9(4)	N(3A)-W(3A)-S(4A)	92.2(4)
W(1)-S(1)-W(2B)	65.5(1)	W(1)-S(3)-W(2A)	65.7(1)
W(1)-S(1)-W(3A)	65.6(1)	W(1)-S(3)-W(3B)	65.5(1)
W(2B)-S(1)-W(3A)	65.7(1)	W(2A)-S(3)-W(3B)	65.3(1)
W(1)-S(2)-W(2A)	65.6(1)	W(1A)-S(4A)-W(2A)	65.7(1)
W(1)-S(2)-W(3A)	65.3(1)	W(1A)-S(4A)-W(3A)	66.3(1)
W(2A)-S(2)-W(3A)	65.3(1)	W(2A)-S(4A)-W(3A)	66.2(1)

^a Symmetry codes: W(1A), S(1A), S(2A), S(3A), N(1A) = (-x, -y, 1 - z). W(2A), W(3A), S(4A), N(2A), N(3A) = (-1 + x, y, z). W(2B), W(3B), S(4B), N(2B), N(3B) = (1 - x, -y, 1 - z).

$Mo_6S_8L_6$ clusters from $MoCl_2$, an excess of NaSH, and NaOBu in refluxing *n*-BuOH-pyridine by McCarley and co-workers.⁴ The authors noted in their article that an excess of the sulfiding agent was necessary in their preparation. This required two 1-week steps, as the product of the reaction was deficient in pyridine and had to be treated with NaSH in pyridine at reflux a second time so crystals of the desired product, $Mo_6S_8(C_5H_5N)_6 \cdot 2C_5H_5N$, could be isolated. This reaction, a novel route to a previously unattainable compound, was not facile and led to a pyrophoric precursor product that was insoluble in noncoordinating solvents and amorphous to X-rays. We have recently explored the applicability of this method to the preparation of the related W_6S_8 congeners and report herein the successful synthesis and structural characterization of the N-ligated cluster complexes $W_6S_8(C_5H_5N)_6$ (**1**) and $W_6S_8(C_9H_{13}N)_6 \cdot 6C_6H_6$ (**2**).

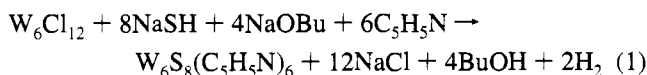
(18) Ehrlich, G. M. Ph.D. Dissertation, Cornell University, Ithaca, NY, 1995, and references therein.

Table 5. Selected Bond Distances (Å) and Angles (deg) in $W_6S_8(C_9H_{13}N)_6 \cdot 6C_6H_6$ (**2**)^a

Bond Distances			
W–W'	2.667(1)	W–S(2 [#])	2.469(2)
W–W''	2.656(1)	W–S(1)	2.459(3)
W–W*	2.667(1)	W–S(2)	2.457(2)
W–W [#]	2.656(1)	W–S(2')	2.458(2)
W–N(1)	2.257(8)		
Bond Angles			
W'–W–W*	60.0(1)	S(1)–W–S(2)	89.3(1)
W''–W–W*	59.9(1)	S(1)–W–S(2')	89.3(1)
W'–W–W [#]	59.9(1)	S(2)–W–S(2 [#])	90.3(1)
W''–W–W [#]	60.3(1)	S(2')–W–S(2 [#])	90.3(1)
W'–W–W''	90.0(1)	S(1)–W–S(2 [#])	172.8(1)
W*–W–W [#]	90.0(1)	S(2)–W–S(2')	173.6(1)
N(1)–W–W'	135.8(2)	N(1)–W–S(1)	95.0(2)
N(1)–W–W''	134.2(2)	N(1)–W–S(2)	93.6(2)
N(1)–W–W*	136.4(2)	N(1)–W–S(2')	92.8(2)
N(1)–W–W [#]	133.6(2)	N(1)–W–S(2 [#])	92.1(2)
W–S(1)–W'	65.7(1)	W–S(2)–W''	65.3(1)
W–S(1)–W*	65.7(1)	W–S(2)–W*	65.7(1)
W'–S(1)–W*	65.7(1)	W''–S(2)–W*	65.2(1)

^a Symmetry codes: ' = (–y, x – y, z), '' = (y, –x + y, –z), * = (–x + y, –x, z), # = (x – y, x, –z).

The $W_6S_8(C_5H_5N)_6$ (**1**) cluster was synthesized from tungsten dichloride, sodium hydrogen sulfide, sodium butoxide, and pyridine in a manner similar to that used for the preparation of $Mo_6S_8(C_5H_5N)_6$,⁴ but employing the following one-pot reaction rather than the two-step sequence needed to obtain the molybdenum cluster:



The red-brown solid obtained from the above reaction was washed with methanol to remove the sodium chloride byproduct and recrystallized from hot pyridine to give cluster **1** as air-stable orange plates. As in the molybdenum case, higher yields were obtainable with an excess of NaSH and a slight excess of the butoxide. In contrast to the molybdenum case, however, no pyrophoric, pyridine-deficient $Na_{2x}W_6S_{8+x}(C_5H_5N)_y$ species were observed or isolated. As expected from the insolubility of $Mo_6S_8(C_5H_5N)_6$,⁴ $W_6S_8(C_5H_5N)_6$ (**1**) is insoluble (at 25°C) in pyridine, acetonitrile, methanol, benzene, toluene, and hexanes.

The ¹³CPMAS solids NMR spectrum for **1** exhibits three unique resonances at δ 123, 135, and 156 ppm which are attributable to the pyridyl meta, para, and ortho carbons, respectively. The corresponding ¹³C values for pyridine (CDCl₃) are δ 123.7, 135.7, and 149.9 ppm.¹³ The larger downfield shift observed for the ortho resonance of **1** is consistent with the metalation of all of the pyridyl nitrogen atoms by tungsten and is similar to that seen for other amine-ligated clusters.⁴ The absence of free, unbound pyridine in **1** was confirmed by a single-crystal X-ray diffraction study (vide infra). The observed and calculated X-ray powder diffraction patterns for **1** are shown in Figure 1. The X-ray powder diffraction pattern of the product exhibits only a few lines at relatively large *d* spacing (small 2θ) at expected positions based on Lazy-Pulverix calculations from the structure reported here.

A model of the structure of $W_6S_8(C_5H_5N)_6$ (**1**), based on a single-crystal X-ray diffraction study, is shown in Figure 2. The structure consists of six tungsten atoms in an octahedral arrangement with eight face capping sulfur atoms. To each tungsten atom is bound a pyridine ligand in the exo position (perpendicular to the cube formed by the S atoms). In the cluster, the W–W–W bond angles, ideally 60°, vary from 59.8

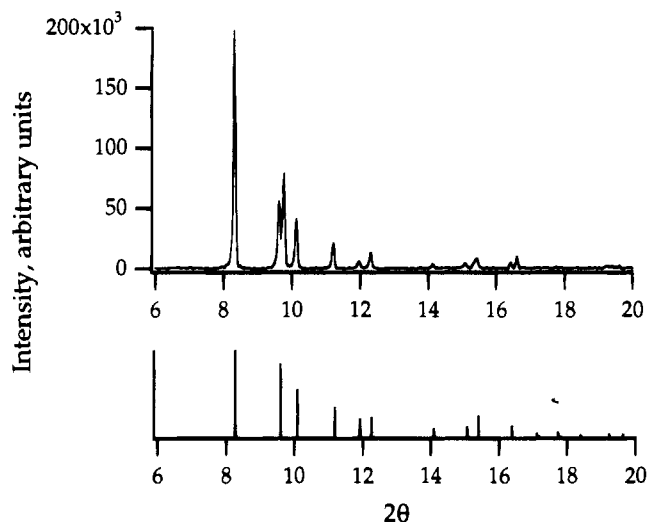


Figure 1. Experimental (top) and calculated (bottom) X-ray powder diffraction patterns for $W_6S_8(C_5H_5N)_6$ (**1**).

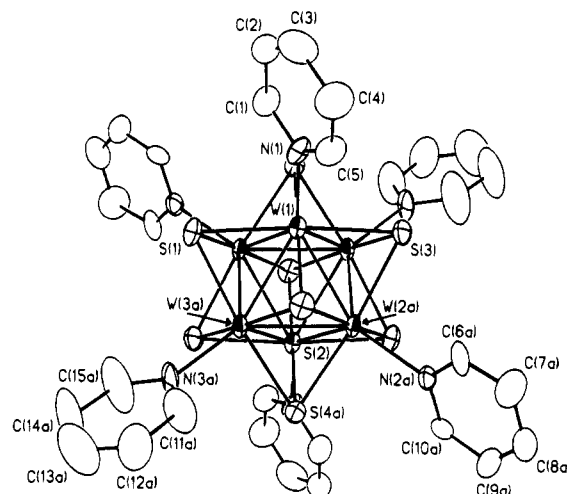
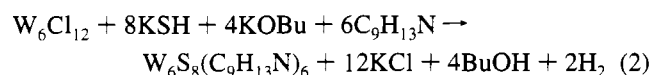


Figure 2. View of $W_6S_8(C_5H_5N)_6$ (**1**) with 50% probability thermal ellipsoids and atomic numbering scheme.

to 60.1°. The W–W bond lengths in the cluster are nearly identical, varying from 2.654(2) to 2.667(2) Å, all of which are shorter than the 2.74 Å W–W bond lengths found in tungsten metal.¹⁹ The W–S bond lengths vary slightly from 2.430(5) to 2.478(4) Å and are comparable to those found in other tungsten sulfide cluster compounds.^{1,2} Similarly, the S–W–S angles are near their ideal values of 90 and 180°; they range from 88.8(2) to 90.4(2)° for the 90° angles and from 172.3(1) to 173.6(2)° for the 180° angles. Consequently, the cluster is slightly distorted from an ideal face-capped octahedron. As one might expect, the pyridine rings are canted relative to each other, most likely in order to facilitate close packing of the clusters in the lattice.

Because of the insolubility of $W_6S_8(C_5H_5N)_6$ and other N-ligated tungsten sulfide clusters in organic solvents, we sought a facile preparation of a W_6S_8 cluster which was soluble in organic solvents to facilitate its use and purification. When tungsten dichloride, potassium hydrogen sulfide, potassium butoxide, and 4-*tert*-butylpyridine are stirred in DMF at room temperature, a dark brown powder can be isolated from the reaction mixture. A balanced chemical equation, similar to that for **1**, can also be written for this reaction:



The reaction can also be run with KH instead of KOBu, but we

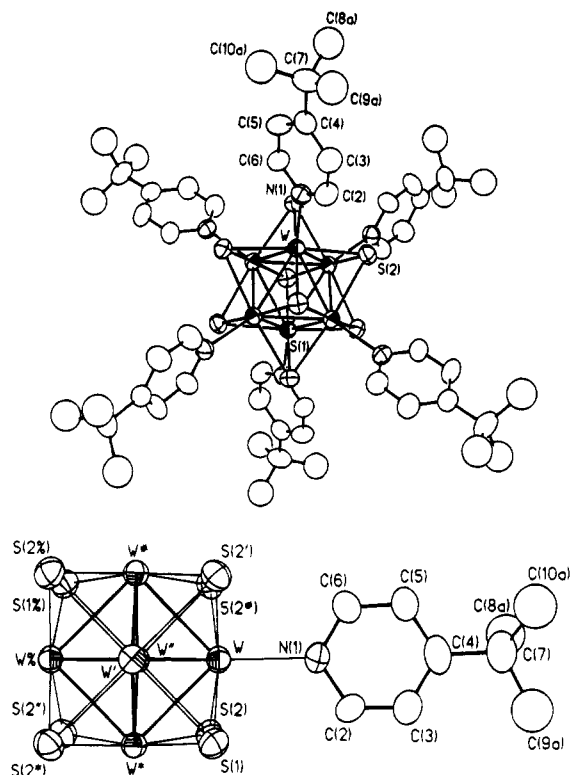


Figure 3. Molecular structure of $W_6S_8(C_9H_{13}N)_6 \cdot 6C_6H_6$ (**2**) with 50% probability thermal ellipsoids and atomic numbering scheme. The benzenes and H atoms have been omitted for clarity, and only the most populated orientation of the disordered 4-*tert*-butyl group is depicted. Top: View approximately down the crystallographic *c* axis. Bottom: Partial view approximately down the $W' \cdots W''$ axis.

have found that this route results in excessive H_2 production (presumably from the reaction of KSH and KH) and a moderate decrease in the overall yield. The KOBu reaction is relatively fast but appears to produce a mixture of products (X-ray powder patterns of solids obtained by stopping the reaction at various times showed the presence of KCl, unreacted KSH, and multiple peaks that could not be assigned to any of the starting materials or presumed product). The $W_6S_8(C_9H_{13}N)_6$ cluster was obtained pure by crystallization from a THF/hexane solvent mixture followed by a second recrystallization from benzene to give **2** or from neat 4-*tert*-butylpyridine at elevated temperatures to give **3**. Both **2** and **3** are soluble in a variety of organic solvents, forming dark orange solutions in THF, DMF, benzene, and DMSO.

The structure of $W_6S_8(C_9H_{13}N)_6 \cdot 6C_6H_6$ (**2**) is shown in Figure 3 (benzene molecules not included). As in **1**, the prototypical W_6S_8 inner core geometry is again observed and encased within an exterior shell of six N-donor ligands (in this case, 4-*tert*-butylpyridines). The latter are terminally bound to the vertices of the W_6 octahedron and are oriented to minimize intramolecular steric repulsions between the pyridyl ortho hydrogens and the core sulfido ligands (Figure 3, bottom). The W_6S_8 cluster is comparable to that in **1** except for a small but statistically significant trigonal distortion. The distortion is expressed as a slight compression of the cluster in the *c* direction, resulting in two faces of the W_6 octahedron being equilateral [$W-W = 2.667(1)$ Å] and the remaining six faces being isosceles [$W-W = 2.656(1)$, $2.656(1)$, and $2.667(1)$ Å]. The occluded benzene molecules within the lattice are involved in only weak ring stacking interactions and are rotationally disordered. These last two observations are consistent with the facile loss of benzene from **2** upon standing (*vide supra*).

The general structural features of **1** and **2** may be compared to those observed in $M_6Cl_8^{4+}$ ($M = Mo, W$)²⁰ and $Mo_6S_8(C_5H_5N)_6 \cdot 2C_5H_5N$.⁴ The average Mo–Mo and W–W bonds in the 24-electron $M_6Cl_8^{4+}$ clusters are 2.6065(1) and 2.607(4) Å, respectively. The average Mo–Mo and W–W bonds in the 20-electron clusters $Mo_6S_8(C_5H_5N)_6 \cdot 2C_5H_5N$, **1**, and **2** are 2.644(2), 2.662(2), and 2.662(6) Å, respectively. Since the distances in the 24-electron clusters may be viewed as effectively single-bond values, Pauling's bond order equation²¹ $d(n) = d(l) - 0.6 \log n$ with $d(l) = 2.6065$ Å (or 2.607 Å) and $n = 20/24$ may be used to estimate the expected Mo–Mo and W–W bond lengths in 20-electron $M_6Cl_8^{8+}$ clusters. The expectation values obtained in this way are 2.654 and 2.655 Å, respectively. The observed range of values [2.644(2)–2.662(6) Å] for the 20-electron Mo_6S_8 and W_6S_8 clusters are in good agreement with these expectation values, suggesting that the expansion of the W_6 core in going from $W_6Cl_8^{4+}$ to W_6S_8 is predominately attributable to the loss of 4 cluster electrons. Conversely, the assumption that charge and size differences between Cl and S are small enough to allow for transferability of the single-bond values from the octachloro to the octasulfido system would appear to be valid. The average M–S bonds are 2.462(3), 2.456(4), and 2.461(3) Å for $Mo_6S_8(C_5H_5N)_6 \cdot 2C_5H_5N$, **1**, and **2**, respectively, while the corresponding M–N bonds are 2.283(9), 2.263(6), and 2.257(8) Å. Interestingly, in spite of a slightly larger W atomic radius, the W–N bonds are consistently shorter than the Mo–N bonds.

In summary, the molecular tungsten sulfide cluster $W_6S_8(C_5H_5N)_6$ (**1**) has been prepared from the reaction of W_6Cl_{12} , NaSH, and NaOBu in refluxing pyridine. This material contains a cluster of six tungsten atoms in an octahedral arrangement with eight face-capping sulfur atoms. Each tungsten atom in the cluster is bound to the nitrogen atom of a pyridine molecule, and there are six of these molecules, each situated perpendicular to one of the S_8 cube faces. The $W_6S_8(C_9H_{13}N)_6 \cdot 6C_6H_6$ (**2**) analog can also be prepared under milder conditions using 4-*tert*-butylpyridine instead of pyridine as a ligand. Cluster **2** has essentially the same structure as **1** but dissolves more readily in a variety of organic solvents making **2** easier to obtain in pure form for use in other synthetic applications.

Note Added in Proof. KSH is hygroscopic and decomposes on exposure to air. In the preparation of $W_6S_8(C_9H_{13}N)_6$, we have found that the purity of the KSH affects the yield of the product. As the purity of the KSH is improved, higher yields are obtained when the reactant ratios are closest to those given in eq 2.

Acknowledgment. The authors thank Dr. Michael Steigerwald for helpful contributions and discussions concerning the synthesis of these tungsten sulfide cluster compounds. This work was supported by the Department of Energy, Basic Energy Sciences, Grant No. DE-FG-02-87ER45298.

Supporting Information Available: Textual presentations of the structure solutions for **2** and **3** and complete tables of experimental crystallographic details, atomic coordinates, anisotropic displacement parameters, and bond distances and angles and additional structural diagrams for **1**–**3** (44 pages). Ordering information is given on any current masthead page.

IC950245Q

- (19) Greenwood, N. N.; Earnshaw, A. *Chemistry of the Elements*; Pergamon Press: New York, 1984; pp 1167–1210.
- (20) (a) Fedin, V. P.; Geras'ko, O. A.; Fedorov, V. E.; Virovets, A. V.; Slovokhotov, Yu. L.; Struchkov, Yu. T. *Zh. Neorg. Khim.* **1990**, *35*, 1142. (b) Zietlow, T. C.; Schaefer, W. P.; Sadeghi, B.; Hua, N.; Gray, H. B. *Inorg. Chem.* **1986**, *25*, 2195.
- (21) Pauling, L. *The Nature of the Chemical Bond*, 3rd ed.; Cornell University Press: Ithaca, NY, 1960; p 400.